DOI: 10.1002/ejic.200500725

Synthesis and Structural Characterisation of Palladium and Group-12 Metal Complexes with a Hybrid Phosphanylphosphonate Ferrocene Ligand

Petr Štěpnička,*[a] Ivana Císařová,[a] and Róbert Gyepes[a]

Keywords: Group 12 metals / Phosphanes / Phosphonate esters / Palladium / Sandwich complexes / Structure eluicidation

Diethyl [1′-(diphenylphosphanyl)ferrocenyl]phosphonate (**1**) was synthesised by stepwise metallation/functionalisation of 1,1′-dibromoferrocene and studied as a ligand for palladium(II) and group-12 metals. Treatment of $[PdCl_2(cod)]$ (cod = η^2:η^2-cycloocta-1,5-diene) with **1** in 1:1 or 1:2 molar ratios gave, respectively, the dinuclear, chloride-bridged complex $[\{Pd(\mu\text{-}Cl)Cl(\mathbf{1}\text{-}\kappa P^2)\}_2]$ (**2**) and the mononuclear complex *trans*-$[PdCl_2(\mathbf{1}\text{-}\kappa P^2)_2]$ (**3**), where **1** coordinates exclusively through the phosphane function. The reactions between **1** and group-12 metal bromides MBr_2 in a 1:1 molar ratio gave the adducts $[MBr_2(\mathbf{1})]$ [M = Zn (**4**), Cd (**5**), and Hg (**6**)], whose crystal structures change considerably with the metal ion. Thus, whereas **4** is a molecular complex with **1** coordinating as an O^1,P^2-chelate, its cadmium(II) analogue is a polymer built up from symmetric $\{CdBr(\mu\text{-}Br)\}_2$ units interconnected by pairs of O^1,P^2-bridging phosphanylphosphonate ligands. Finally, the mercury(II) complex **6** is a halide-bridged dimer, $[\{Hg(\mu\text{-}Br)Br(\mathbf{1}\text{-}\kappa P^2)\}_2]$. However, this compound is structurally fluxional in solution (NMR spectra) and, in the crystal, it attains a structure similar to **5** owing to weak interactions between mercury and phosphonate-O^1 atoms from adjacent molecules. An isomer to **6**, $[\{HgBr_2(\mathbf{1}\text{-}\kappa^2 O^1,P^2)\}_2]$ (**7**), was isolated from attempted alkylation of **6** and structurally characterised as a dimer, where ligands **1** bridge two $\{HgBr_2\}$ units. All compounds were studied by spectroscopic methods (IR, NMR, mass) and the solid-state structures of **1**, **2**·½H_2O, **3**·4 $CHCl_3$, **4**, **5**, **6**·5 C_6H_6, and **7** have been determined by single-crystal X-ray diffraction.

Introduction

Ferrocene donors have attracted considerable attention as valuable ligands for coordination compounds and catalytic applications. Among the numerous multidentate ferrocene donors that have been synthesised during the last few decades, chiral, mixed-donor (typically PN) ligands derived from a 1,2-disubstituted ferrocene backbone have proved to be particularly successful.[1] In contrast, the related unsymmetrical, 1,1′-disubstituted ferrocene derivatives have been studied much less.[2] This applies particularly to donors whose asymmetry arises from the presence of two different phosphorus groups. To date only a few ferrocene diphosphanes Ph_2PfcPR_2 {fc = ferrocene-1,1′-diyl; PR_2 = PPh(*t*Bu),[3] P(*t*Bu)$_2$,[4] and $P(C_6H_4Y\text{-}4)_2$, Y = OMe, CF_3[5]}, phosphanylphosphonites $Ph_2PfcP(OR)_2$,[6] and dppf semi-chalcogenides $Ph_2PfcP(E)R_2$ (E = O,[7] S, and Se[8]) have been reported in the literature, which stands markedly against the vast chemistry of the "popular", symmetric ferrocene diphosphane 1,1′-bis(diphenylphosphanyl)-ferrocene (dppf).[9]

Recent interest in the synthesis and coordination chemistry of ferrocene phosphonate esters and acids[10] led us to design the ferrocene phosphanylphosphonate ligand $Ph_2PfcP(O)(OEt)_2$ (**1**) and study its coordination behaviour. In this contribution, we report the synthesis, characterisation and structures of this ligand and its complexes with palladium(II) and group-12 metals. It should be noted that compound **1** was reported as an intermediate in the synthesis of diphosphanes Ph_2PfcPH_2 and Ph_2PfcPR_2 [PR_2 = (*R*,*R*)-2,5-dimethylphospholan-1-yl] while this work was in progress.[11] However, no investigation into its donor properties was mentioned.

Results and Discussion

Diethyl [1′-(diphenylphosphanyl)ferrocenyl]phosphonate (**1**) was prepared by lithiation of 1-bromo-1′-(diphenylphosphanyl)ferrocene followed by addition of diethyl chlorophosphate to the formed lithio intermediate, using the general methodology developed by Butler et al.[7a] Subsequent chromatography of the crude product contaminated with (diphenylphosphanyl)ferrocene and some other minor impurities on alumina furnished a good yield of pure **1** as an amber oil, which slowly crystallised upon standing at room temperature (faster at +4 °C) to give an orange, waxy solid. The compound was characterised by standard spectroscopic methods and its structure determined by X-ray diffraction analysis (see Figure 1 and the section dealing with the crystal structures below). It was then studied as a ligand in palladium(II) and group-12 metal complexes.

[a] Department of Inorganic Chemistry, Faculty of Science, Charles University,
Hlavova 2030, 12840 Prague, Czech Republic
E-mail: stepnic@natur.cuni.cz
Supporting information for this article is available on the WWW under http://www.eurjic.org or from the author.

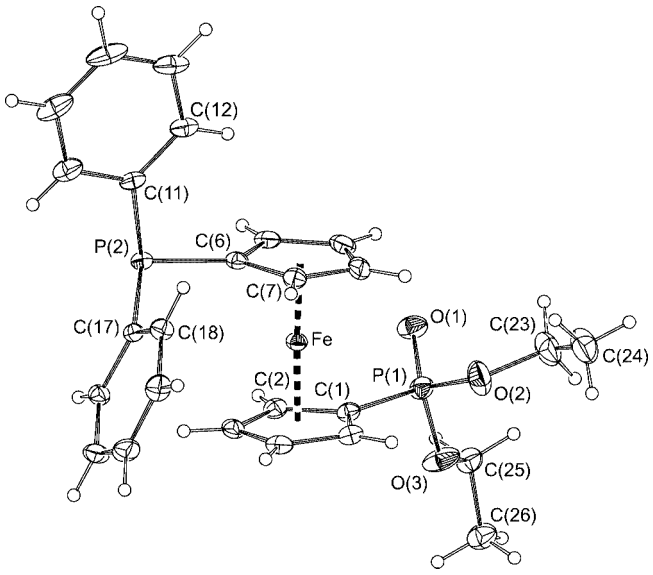

Figure 1. Molecular structure of **1** showing the atom-labelling scheme; for the consecutively numbered ring atoms, only labels of the pivotal atom and its adjacent ring carbon atoms are shown for clarity (note: the atom-numbering scheme adopted for the ligand moieties in all complexes is similar). Displacement ellipsoids are scaled to the 30% probability level. Selected distances [Å] and angles [°]: Fe–Cg(1) 1.6488(9), Fe–Cg(2) 177.00(5), P(1)–O(1) 1.467(2), P(1)–O(2) 1.587(2), P(1)–O(3) 1.572(2), P(1)–C(1) 1.761(2), P(2)–C(6) 1.813(2), P(2)–C(11) 1.838(2), P(2)–C(17) 1.831(2); Cg(1)–Fe–Cg(2) 177.00(5), range of O–P(1)–O angles 105.9(1)–115.7(1), range of C(1)–P(1)–O angles 98.59(9)–117.7(1), range of C–P(2)–C angles: 100.88(9)–102.13(8), ∠ Cp1,Cp2 4.5(1)°, τ[C(1)–Cg(1)–Cg(2)–C(6)] = 155.2(1)°; Cg(1) and Cg(2) are the centroids of the cyclopentadienyl rings C(1–5) (Cp1) and C(6–10) (Cp2), respectively.

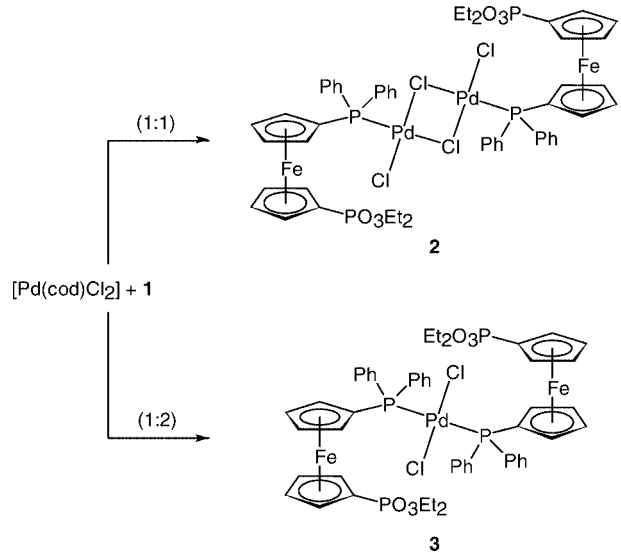

Scheme 1.

Palladium(II) Complexes

Depending on the stoichiometry, the reaction of [Pd(cod)Cl_2] (cod = η^2:η^2-cycloocta-1,5-diene) with **1** gives either the chloride-bridged dipalladium(II) complex *trans*-[{Pd(μ-Cl)Cl(**1**-κP^2)}$_2$] (**2**) or the bis(phosphane) complex *trans*-[$PdCl_2$(**1**-κP^2)$_2$] (**3**; Scheme 1). Attempted removal of the chloride ligands from **3** by treatment with $AgClO_4$ gave an intractable, dark-red, oily residue that shows broad signals in the NMR spectra.

The reaction in a 1:1 molar ratio in methanol produced a dark-red, crystalline solid, which was structurally characterised as *trans*-[{Pd(μ-Cl)Cl(**1**-κP^2)}$_2$] (**2**). The spectroscopic data for **2** give no clear signs about the coordination mode of the phosphanylphosphonate ligand and do not allow us to distinguish between two possible isomeric forms, namely **2** and [$PdCl_2$(**1**-κ$^2O^1$,P^2)]. For instance, the ^{1}H NMR spectra exhibit markedly downfield-shifted ferrocene signals (as compared to **1** and **3**) but practically unaffected signals for the ethoxy groups [$\Delta\delta_H(CH_2) \approx +0.03$ ppm] whilst the ^{31}P NMR spectra show two distinct signals at δ_P = 24.6 and 31.1 ppm due to the phosphonate and phosphanyl groups, respectively {coordination shifts [$\Delta\delta_P$ = δ_P(complex) – δ_P(ligand)] of 48.1 (P^{III}) and –1.1 ppm (P^V), recorded in $CDCl_3$}.

More information about the structure of **2** was obtained from the far-IR spectrum, which contains a strong band at 356 cm^{-1} (with shoulder at 350 cm^{-1}), and several bands at 249–256 cm^{-1} attributable to ν(PdCl) stretching vibrations involving the terminal and bridging chloride ligands, respectively. An unambiguous proof of the compound structure came from the X-ray diffraction analysis (Figure 2). Crystals amenable to the diffraction analysis were obtained directly from the reaction mixture. However, since the poor quality of the available crystals (disorder of the phosphonate group and crystal defects) resulted in a relatively low overall quality of the structural data, only the most important structural features will be addressed here.[12]

The structure determination for **2** revealed a doubly halide-bridged dimeric structure with a *sym-trans* geometry. Remarkably, the dihedral angle subtended by the {$PdCl_2P$} least-squares planes is as high as 40.91(5)°, which is rather uncommon for compounds of this type. A search in the Cambridge crystallographic database[13] revealed that the observed tilting of the coordination planes is among the highest observed.[14] As expected, the Pd–Cl bonds to terminal chlorides (2.27 Å) are significantly shorter than those to bridging ones (2.33–2.44 Å). The Pd–P bonds in **2** are about 0.12 Å shorter than those in **3** (see below), which can be ascribed to a lower *trans* influence of the chloride ligand in comparison with the phosphane donor, and possibly also to a less sterically strained structure of **2** where the two bulky phosphanylphosphonate ligands are separated by the Pd(μ-Cl)$_2$Pd core.

For complex **3**, which is formed at a 2:1 ligand-to-metal ratio, the exclusive P-coordination of **1** is clearly manifested by a considerable shift to lower fields for the phosphanyl signal and practically unaffected phosphonate resonance [$\Delta\delta_P(P^{III})$ = 32.3 ppm/$\Delta\delta_P(P^V)$ = –0.6 ppm]. The ^{31}P coordination shifts for the palladium complexes reflect a relatively higher *trans* influence of the phosphane donor (see also

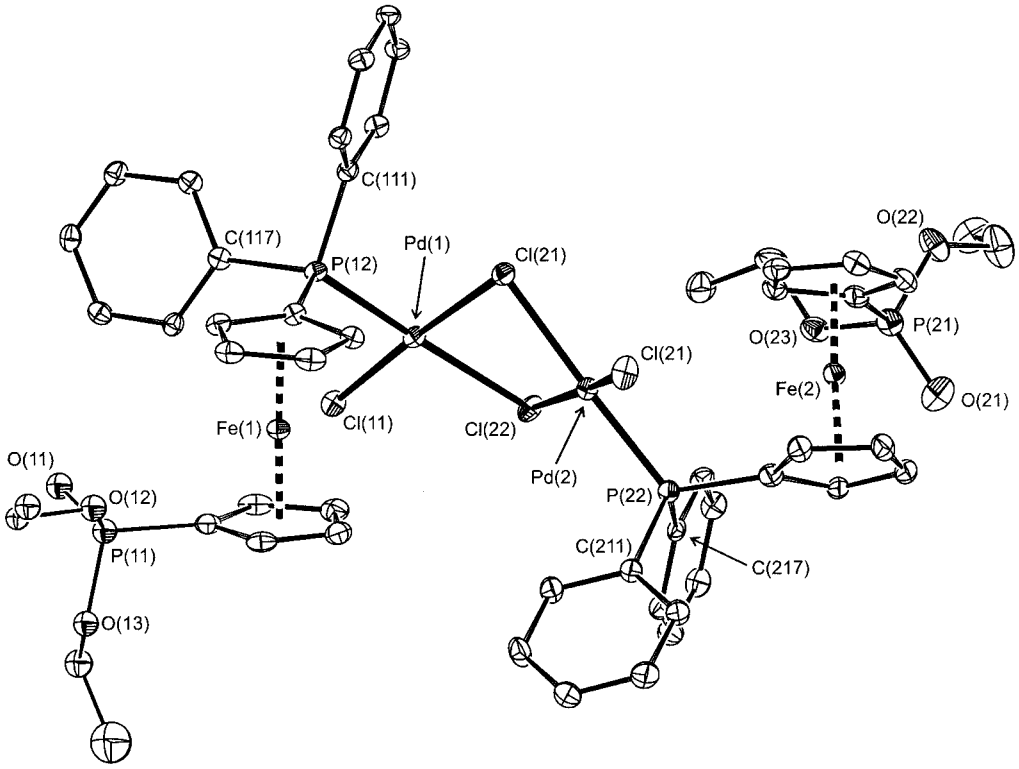

Figure 2. A view of the structure of complex **2** as determined for the solvate **2**·½H_2O. For clarity, the solvating water molecule and hydrogen atoms have been omitted and only one orientation of the disordered phosphonate group [the group involving the P(11) atom] is shown. Displacement ellipsoids are drawn at the 20% probability level. The atom-numbering scheme is analogous to that of **1**; the first digit is added to distinguish the symmetrically independent molecular parts. Selected distances [Å] and angles [°]: Pd(1)–Cl(11) 2.273(2), Pd(1)–Cl(12) 2.329(2), Pd(1)–Cl(22) 2.443(2), Pd(1)–P(12) 2.229(2), Pd(2)–Cl(21) 2.273(2), Pd(2)–Cl(12) 2.415(2), Pd(2)–Cl(22) 2.325(2), Pd(2)–P(22) 2.227(2); Cl(11)–Pd(1)–Cl(22) 92.48(5), Cl(11)–Pd(1)–P(12) 93.54(6), Cl(12)–Pd(1)–Cl(22) 83.88(5), Cl(12)–Pd(1)–P(12) 90.06(6), Cl(12)–Pd(2)–Cl(21) 91.70(6), Cl(12)–Pd(2)–Cl(22) 84.58(6), Cl(21)–Pd(2)–P(22) 88.19(7), Cl(22)–Pd(2)–P(22) 95.85(6), Pd(1)–Cl(12)–Pd(2) 89.50(6), Pd(1)–Cl(12)–Pd(2) 88.92(5).

above), which causes the ^{31}P NMR resonance to shift to higher field.[16] Simple phosphanes behave similarly; see, for instance, the pair of related complexes *trans*-[{Pd(μ-Cl)-Cl(L)}$_2$] ($\Delta\delta_P$ = 39.5 ppm) and *trans*-[$PdCl_2L_2$] ($\Delta\delta_P$ = 29.4 ppm), where L is tri-*p*-tolylphosphane.[15]

The ^1H NMR spectra of **3** spectra exhibit a shift to lower field for all ferrocene signals but virtually no change for the phosphonate ethoxy groups. The ^{13}C NMR spectrum displays resonances due to the carbon atoms at the phosphanyl-substituted cyclopentadienyl and phenyl rings as virtually coupled triplets arising from ABX spin systems [^{12}C-$^{31}P(A)$-(metal)-$^{31}P(B)$-$^{13}C(X)$] with relatively large $J_{A,B}$ values.[16] Very similar features have been observed for the related complex with P-monodentate 1′-(diphenylphosphanyl)ferrocenecarboxylic acid (Hdpf), *trans*-[$PdCl_2$(Hdpf-κ*P*)$_2$].[17] The solid-state structure of the solvate **3**·4$CHCl_3$ was determined by single-crystal X-ray diffraction analysis (see below).

Group-12 Metal Complexes

Mixing the phosphanylphosphonate **1** with bromides of divalent group-12 metals in a 1:1 molar ratio in acetone and subsequent crystallisation by diffusion of diethyl ether vapour gave adducts [MBr_2(**1**)] [M = Zn (**4**), Cd (**5**), and Hg (**6**)] as air-stable, yellow-orange, crystalline solids.[18] However, the exact formulation for these compounds as based on spectral evidence and crystallographic data (see below) is rather complex and differs for all the members of the series. Thus, whereas compound **4** is a monomeric tetrahedral complex featuring **1** as an *O*,*P*-chelating donor, [$ZnBr_2$(**1**-κ$^2O^1$,P^2)], its cadmium analogue is a coordination polymer in which dinuclear {Cd(μ-Br)Br}$_2$ units are linked into infinite chains by means of symmetric pairs of the O^1,P^2-bridging phosphanylphosphonate ligands (see Scheme 2). This is reflected also by the very poor solubility of **5** compared to the well soluble **4** and **6**.

The ^{31}P NMR spectrum of **4** is clearly indicative of *O*,*P*-chelate coordination by showing a pair of doublets at δ_P = –19.9 and 26.1 ppm ($^3J_{P,P}$ = 5 Hz) assignable to the mutually coupled phosphane and phosphonate phosphorus atoms, respectively. The coordination shifts ($\Delta\delta_P$) of –2.9 (P^{III}) and +0.4 (P^V) ppm correspond favourably with the shifts observed for [$ZnCl_2$L] complexes with *P*,*P*′-chelating symmetric ferrocene diphosphanes [L/$\Delta\delta_P$ = dppf/–4.5 ppm,[19] and dippf/–6.6 ppm; dippf = 1,1′-bis(diisopropylphosphanyl)ferrocene],[20] and a complex containing two O^1-monodentate diethyl ferrocenylphosphonate ligands,

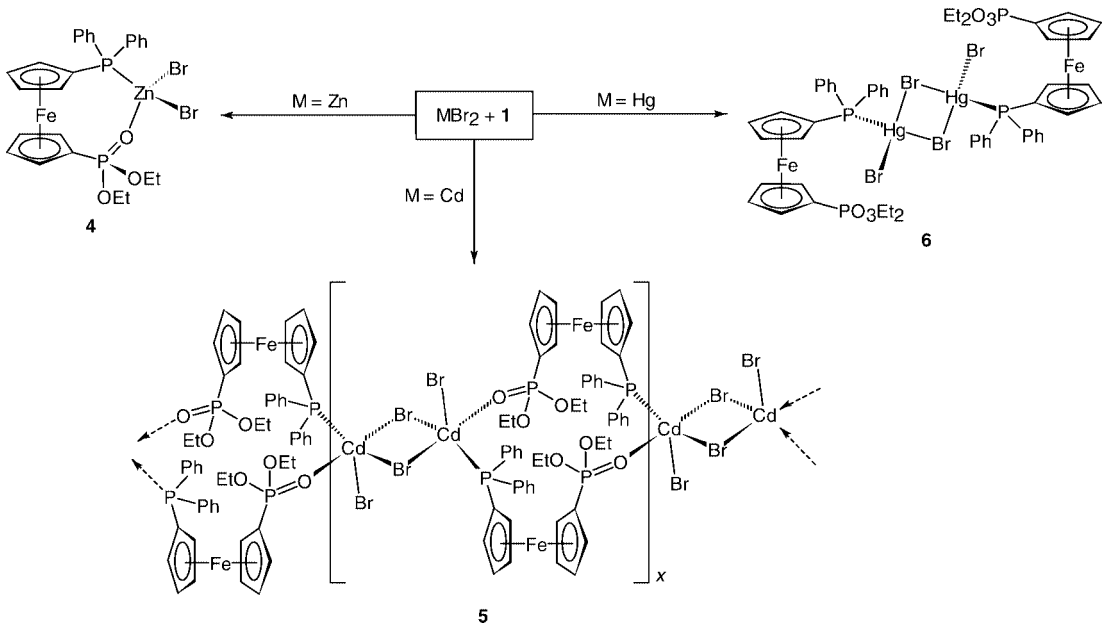

Scheme 2. Schematic drawing of structures of the products arising from group-12 metal dibromides and **1**. For compound **5**, the arrows indicate where propagation of the one-dimensional infinite polymeric chain occurs.

$[ZnCl_2\{FcPO_3Et_2\text{-}\kappa O^1\}_2]$ ($\Delta\delta_P$ = +0.7 ppm in CD_3OD, Fc = ferrocenyl).[10c] Furthermore, the coordination of the phosphonate group is manifested by a shift of the multiplet due to the OCH_2 protons by about 0.3 ppm to lower field in the ^1H NMR spectrum.

The IR spectra of **4** and **5** in the region down to about 300 cm^{-1} exhibit mostly bands due to the ligand; useful information about the coordination geometry is provided by the far-IR region. In the case of **4**, two bands attributable to symmetric and antisymmetric ν(ZnBr) stretching vibrations are observed at 219 and 251–254 cm^{-1}, respectively, close to the values reported for $[ZnBr_2(PPh_3)_2]$ (236 and 205 cm^{-1}).[21] The far-IR spectrum of **5** exhibits a pair of bands as well (at 193 and 158 cm^{-1}). The positions of these bands assignable to ν(CdBr) stretching vibrations involving terminal and bridging bromide atoms correspond to those of the binuclear, halide-bridged complex $[\{Cd(\mu\text{-}Br)Br(PCy_3)\}_2]$, which, however, features only tetracoordinate cadmium centres (208 and 169–144 cm^{-1}).[22] Notably, the ν(ZnBr)/ν(CdBr) ratios for the band pairs (1.31 and 1.39) correspond well to the expected value obtained from the mass factor: $[A_r(Cd)/A_r(Zn)]^{1/2} \approx 1.31$.

As revealed by X-ray analysis, compound **6** is a symmetric, halide-bridged dimer with the ligand coordinating as a simple phosphane: $[\{Hg(\mu\text{-}Br)Br(\mathbf{1}\text{-}\kappa P^2)\}_2]$ (Scheme 2). The solution NMR spectroscopic data, particularly the relatively large $^1J_{Hg,P}$ coupling constant and the coordination shift $\Delta\delta_P(P^{III})$ of 41.4 ppm, indicate that this structure is most likely retained in solution (cf. the parameters for $[HgBr_2(PPh_3)_2]$ ($^1J_{Hg,P}$ = 4240 Hz/$\Delta\delta_P$ = 27.3 ppm) and $[\{Hg(\mu\text{-}Br)Br(PPh_3)\}_2]$ ($^1J_{Hg,P}$ = 6450 Hz/$\Delta\delta_P$ = 32.6 ppm) recorded in $CDCl_3/CH_2Cl_2$, 1:1[23]). However, a detailed NMR study revealed a fluxional behaviour in solution: the spectra of **6** change with temperature, solvent and also with the sample concentration (see Table 1 and Figures S1 and S2 in the Supporting Information). Upon raising the sample temperature, the signal due to the phosphane group (P^{III}) in the ^{31}P NMR spectrum shifts to lower fields while the coupling to ^{199}Hg increases. In contrast, the phosphonate resonance moves upfield with increasing temperature. In the ^1H NMR spectrum the major change occurs in the region of the ferrocene cyclopentadienyl resonances: the signals due to the phosphonate ethoxy groups exhibit practically constant chemical shifts (note that the multiplet of the methylene group is not entirely invariant as it becomes better resolved at *higher* temperatures).

Table 1. Variable temperature (VT) $^{31}P\{^1H\}$ NMR spectroscopic data for **6**.[a]

T [°C]	$\delta(P^V)$ [ppm]	$\delta(P^{III})$ [ppm]	$^1J_{Hg,P^{III}}$ [Hz]
+50	23.73	–	–[b]
+25	23.88	24.38	6587
0	24.06	23.69	6702
–25	24.22	23.52	6809
–50	24.35	23.02	6908
+25[c]	23.88	24.56	6560

[a] The spectra were recorded for a 0.036 M solution in $CDCl_3$. The VT ^1H and $^{31}P\{^1H\}$ NMR spectra are available as Supporting Information (see Figures S1 and S2, respectively). Reference data for **1**: δ_P = –17.0 (P^{III}) and 25.7 ppm (P^V) (in $CDCl_3$ at 25 °C). [b] Not detected due to signal broadening. [c] Data for a 0.018 M solution.

These spectral characteristics resemble in some respects the solution behaviour of the phosphane complexes $[HgX_2(PR_3)_2]$,[23] and are clearly indicative of structural fluxionality. Considering the NMR and structural data (see below), as well as the donor ability of the ligand, the dynamic processes occurring in solutions of $[HgBr_2(\mathbf{1})]$ may

be formulated as shown in Scheme 3. One may expect the hybrid donor **1** to coordinate to the soft mercury atom more strongly through its phosphane group than through the phosphonate oxygen. The inherent weakness of Hg–O bonds would facilitate the formation of tricoordinate species **I** which, in turn, can give rise to intermediate **II** (by closure of the *O*,*P*-chelate ring with the Hg–P bond acting as a pivot) or, by dimerisation, to the halide (**6**) or *O*,*P*-**1**-bridged (**7**) dimers. As mentioned above, the NMR spectroscopic data indicate that the solution equilibrium is shifted in favour of dimer **6**. However, since solvent, concentration and temperature influence the overall distribution, individual components may separate from solutions of [$HgBr_2$(**1**)] depending on their relative solubility in the reaction media (see the structure of **7** below).

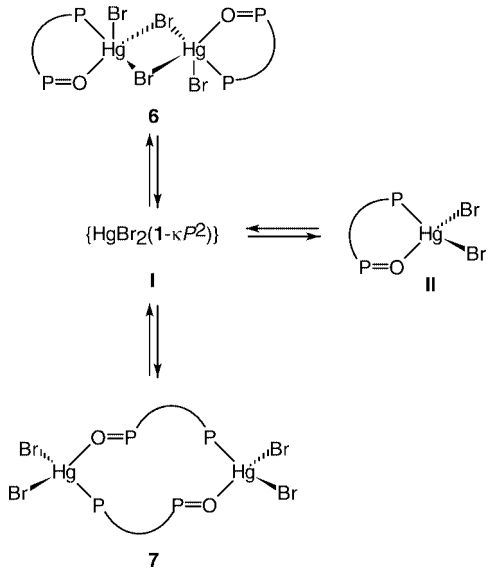

Scheme 3. Schematic depiction of the exchange equilibria of [$HgBr_2$(**1**)].

Crystal Structures

The crystal structure of the solvate **3**·4$CHCl_3$ (Figure 3, Table 2) corroborates the expected *trans* square-planar coordination of the palladium atom. The molecule of the complex is perfectly planar and centrosymmetric due to the imposed crystallographic symmetry. Nevertheless, owing to the steric bulk of the P-bonded (diphenylphosphanyl)ferrocenyl ligands, the interligand angles deviate slightly from the ideal value of 90°. The ferrocene units in **3** are rotated with respect to the coordination plane by approximately 53°, which seems to minimise the steric interactions of the bulky phosphane ligands by bringing the "PC_3" moieties of the phosphanylferrocene ligands into a close-to-staggered conformation. This coordination geometry seems to be common to all structurally characterised complexes involving 1′-functionalised ferrocene phosphanes: *trans*-[$PdCl_2$(Ph_2PfcX-κ*P*)], where X = CO_2H,[17] $P(O)Ph_2$,[24] SMe,[25] and (*S*)-4-isopropyl-4,5-dihydrooxazolyl-1-yl.[26]

Table 2. Selected bond lengths [Å] and angles [°] for **2**·4$CHCl_3$.[a]

Pd–Cl	2.2984(7)	Cl–Pd–P(2)	86.71(2)
Pd–P(2)	2.3467(6)	Cl–Pd–P(2^i)	93.29(2)
P(1)–O(1)	1.467(3)	O–P(1)–O[b]	101.3(2)–115.3(2)
P(1)–O(2)	1.572(3)	C(1)–P(1)–O[c]	100.4(1)–115.6(2)
P(1)–O(3)	1.593(3)	Pd–P(2)–C[d]	110.89(9)–121.1(1)
P(1)–C(1)	1.755(3)	C–P(2)–C[e]	102.3(1)–104.8(1)
P(2)–C(6)	1.802(3)		
Fe–Cg(1)	1.650(1)	∠ Cp1,Cp2	2.7(2)
Fe–Cg(2)	1.650(1)	τ[f]	–135.8(2)

[a] Symmetry operations used to generate equivalent positions: *i*: –*x*, –*y*, 2 – *z*. Definition of the ring planes: Cp1: C(1–5); Cp(2): C(6–1). Cg(1) and Cg(2) are the respective ring centroids. [b] The range of O(1)–P–O(2,3) and O(2)–P(1)–O(3) angles. [c] The range of C(1)–P(1)–O(1,2,3) angles. [d] The range of Pd–P(2)–C(6,11,17) angles. [e] The range of C(6)–P(2)–C(11,17) and C(11)–P(2)–C(17) angles. [f] Torsion angle C(1)–Cg(1)–Cg(2)–C(6).

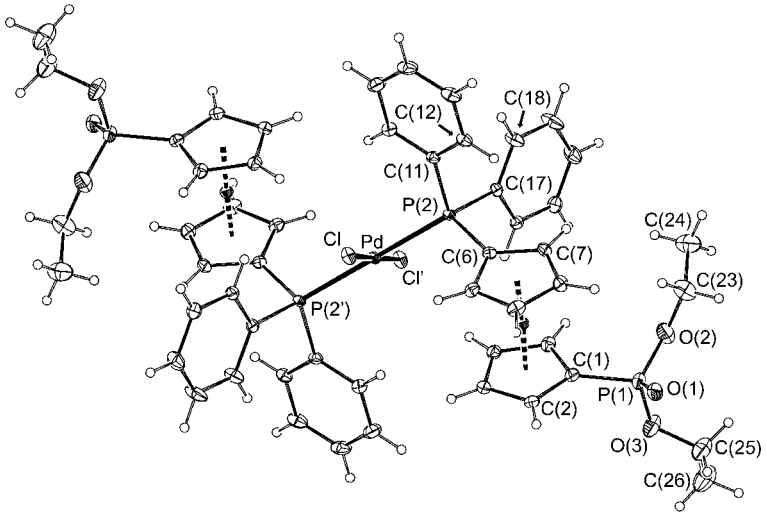

Figure 3. Molecular structure of **3**·4$CHCl_3$. Displacement ellipsoids are drawn at the 30% probability level; the solvate molecules have been omitted for clarity. Half of the molecule is generated by a (crystallographic) inversion operation, the centre of which coincides with the palladium atom.

The ligand phosphonate groups, which do not participate in coordination, are rotated away from the phosphanyl substituent such that the disubstituted ferrocene framework adopts a conformation near to anti-eclipsed with a τ angle of 136° (cf. the ideal value of 144°). Due to the symmetry of the crystal assembly, the phosphonate groups in individual molecules are inclined towards each other, forming polar domains that accommodate the solvate: each phosphonate moiety binds two solvent molecules by O···H–CCl_3 hydrogen bonds to its phosphoryl oxygen atom [C(80)–H(80)···O(1^i): C(80)···O(1^i) 3.134(5) Å, angle at H(80) 147°; C(90)–H(90)···O(1^i): C(90)···O(1^i) 3.014(5) Å, angle at H(80) 167°; i (x, 1 + y, z). Consequently, the overall crystal packing can be described as molecular, built up from {**2**$(CHCl_3)_4$} repeating units.

As mentioned above, the solid-state structures of 1:1 complexes involving all group-12 metals [MBr_2(**1**)] [M = Zn (**4**), Cd (**5**) and Hg (**6**)] were established by single-crystal X-ray diffraction. Furthermore, an isomer of the latter compound (denoted as **7**, Scheme 3) was also structurally characterised. Crystals of **7** suitable for diffraction analysis were obtained from an attempted alkylation of **6** with iodomethane in methanol, followed by evaporation and crystallisation of the residue from acetone/diethyl ether. Although the IR and solution NMR spectra of the bulk material are virtually identical with the starting material **6**, their crystal structures differ markedly. Structural drawings for **4**–**7** are shown below; selected structural parameters are listed in the appropriate tables.

Clearly, the structures change with the metal and are dictated by a subtle interplay between the hardness of the central atom and the donor abilities of the functional groups available at the ferrocene ligand. With zinc, the smallest and hardest (though polarizable) metal in group 12, the ligand coordinates through both donor groups to form a molecular chelate (Figure 4, Table 3). The unit cell of **4** contains two symmetrically independent but structurally very similar molecules of the complex that differ slightly in the mutual orientation of the ferrocene ligand and the embedded $ZnBr_2$ motif, and further by conformation of the flexible ferrocene, phenyl and ethoxy groups. The coordination spheres around the zinc atoms in both molecules are quite regularly tetrahedral, albeit with rather varying zinc–donor distances: the coordination mode can be described as [3+1] with Zn–Br ≈ Zn–P > Zn–O. The individual bond lengths are comparable with the data reported for

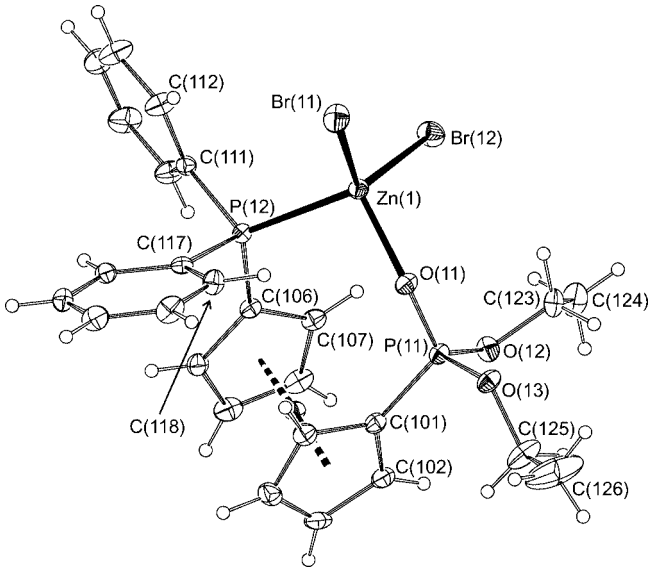

Figure 4. A view of the molecular structure of complex **4** (molecule 1). Displacement ellipsoids enclose 30% probability. Atom labels for molecule 2 (see text) are obtained by adding one to the first digit of the respective atom label in molecule 1.

Table 3. Selected bond lengths [Å] and angles [°] for **4**.[a]

Molecule 1		Molecule 2	
Zn(1)–Br(11)	2.3602(5)	Zn(2)–Br(21)	2.3661(5)
Zn(1)–Br(12)	2.3401(5)	Zn(2)–Br(22)	2.3636(5)
Zn(1)–P(12)	2.4097(8)	Zn(2)–P(22)	2.4249(8)
Zn(1)–O(11)	2.008(2)	Zn(2)–O(21)	2.004(2)
P(11)–O(11)	1.479(2)	P(21)–O(21)	1.481(2)
P(11)–O(12)	1.559(2)	P(21)–O(22)	1.551(2)
P(11)–O(13)	1.577(2)	P(21)–O(23)	1.571(2)
P(11)–C(101)	1.757(3)	P(21)–C(201)	1.747(3)
P(12)–C[b]	1.794(3)–1.824(3)	P(12)–C[c]	1.800(3)–1.825(3)
Angles at Zn(1)	101.44(6)–116.85(2)	angles at Zn(2)	99.17(6)–115.73(2)
Zn(1)–O(11)–P(11)	144.0(1)	Zn(2)–O(21)–P(21)	145.3(1)
O–P(11)–O[d]	101.8(1)–116.4(1)	O–P(21)–O[e]	101.5(1)–116.7(1)
C–P(12)–C[f]	103.6(1)–106.8(1)	C–P(22)–C[g]	104.5(1)–107.9(1)
Fe(1)–Cg(11)	1.650(1)	Fe(2)–Cg(21)	1.645(2)
Fe(1)–Cg(21)	1.647(1)	Fe(2)–Cg(21)	1.648(2)
∠ Cp(11),Cp(12)	2.9(2)	∠ Cp(21),Cp(22)	1.8(2)
τ(1)[h]	53.0(2)	τ(2)[i]	–60.2(2)

[a] Definitions of the ring planes: Cp(11) C(101–105), Cp(12) C(106–110), Cp(21) C(201–205), Cp(22) C(206–210). Cg(*ij*) denotes the respective ring centroid. [b] The range of P(12)–C(106,C111,C117) bond lengths. [c] The range of P(22)–C(206,C211,C217) bond lengths. [d] The range of O(11)–P(11)–O(12,13) and O(12)–P(11)–O(13) angles. [e] The range of O(21)–P(21)–O(22,23) and O(22)–P(21)–O(23) angles. [f] The range of C(106)–P(12)–C(111,117) and C(111)–P(12)–C(117) angles. [g] The range of C(206)–P(22)–C(211,217) and C(211)–P(22)–C(217) angles. [h] Torsion angle C(101)–Cg(11)–Cg(12)–C(106). [i] Torsion angle C(201)–Cg(21)–Cg(22)–C(206).

$[ZnCl_2\{FcP(O)(OEt)_2\text{-}\kappa O^1\}_2]$ [Zn–O 1.978(4), P=O 1.467(4), P–OEt 1.555(4) and 1.568(4), P–C 1.770(6) Å][10c] and $[ZnCl_2(dippf\text{-}\kappa^2 P,P')]$ (Zn–P av. 2.415 Å).[20b]

The solid-state structure of cadmium complex **5** (Figure 5) is relatively complicated (Scheme 2, Table 4). Formally, the "$CdBr_2$" units associate into dimers through two bromide bridges. In addition, each cadmium atom is coordinated to two phosphanylphosphonate ligands (once through P=*O* and once through *P*Ph_2) and thus has a coordination number of five. The dicadmium $\{Cd_2Br_4\}$ units are interconnected by means of symmetric ligand pairs to form infinite one-dimensional ribbons (Scheme 2; see also Figure 6).

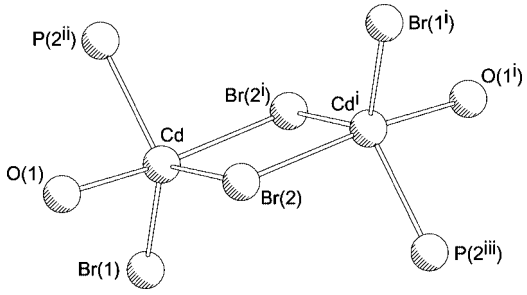

Figure 5. A view of the dicadmium core in **5**. Atomic radii correspond to the isotropic displacement parameters (U_{iso}); symmetry codes: *i*: 1 – *x*, 1 – *y*, –*z*; *ii*: 1 – *x*, 1 – *y*, 1 – *z*; *iii*: *x*, *y*, *z* – 1.

Table 4. Selected bond lengths [Å] and angles [°] for **5**.[a]

Cd–Br(1)	2.5556(4)	O(1)–Cd–Br(2^i)	167.50(5)
Cd–Br(2)	2.6458(4)	O(1)–Cd–Br(1)	94.82(5)
Cd–Br(2^i)	2.8373(3)	O(1)–Cd–Br(2)	86.82(5)
Cd–P(2^{ii})	2.6306(7)	O(1)–Cd–P(2^{ii})	87.60(5)
Cd–O(1)	2.394(2)	Br(2^i)–Cd–Br(1)	97.05(1)
Cd···Cd^i	4.0737(3)	Br(2^i)–Cd–Br(2)	84.10(1)
P(1)–O(1)	1.481(2)	Br(2^i)–Cd–P(2^{ii})	89.41(2)
P(1)–O(2)	1.571(2)	Br(1)–Cd–Br(2)	118.44(1)
P(1)–O(3)	1.566(2)	Br(1)–Cd–P(2^{ii})	122.06(2)
P(1)–C(1)	1.771(3)	Br(2)–Cd–P(2^{ii})	119.50(2)
P(2)–C[b]	1.804(2)–1.823(3)	O–P(1)–O[c]	100.3(1)–115.0(1)
		C–P(2)–C[d]	103.2(1)–104.5(1)
Fe–Cg(1)	1.648(2)	∠ Cp(1),Cp(2)	1.3(2)
Fe–Cg(2)	1.643(2)	τ(1)[e]	–155.9(2)

[a] Definitions of the ring planes: Cp(1) C(1–5), Cp(2) C(6–10); Cg(*i*) denotes the respective ring centroid. Symmetry operations used to generate equivalent positions: *i*: 1 – *x*, 1 – *y*, –*z*; *ii*: 1 – *x*, 1 – *y*, 1 – *z*. [b] The range of P(2)–C(6,11,17) bonds lengths. [c] The range of O(1)–P(1)–O(2,3) and O(2)–P(1)–O(3) angles. [d] The range of C(6)–P(2)–C(11,17) and C(11)–P(2)–C(17) angles. [e] Torsion angle C(1)–Cg(1)–Cg(2)–C(6).

The dicadmium core in **5** (Figure 5) is centrosymmetric and its geometry is best described as two identical trigonal bipyramids sharing an edge connecting the axial and equatorial positions. Because of the steric demands of the ligands and the different cadmium–donor distances [Cd–O(1^i) < Cd–Br(1) < Cd–P(2^{ii}) ≈ Cd–Br(2) < Cd–Br(2^i); for symmetry codes, see Figure 5], the trigonal bipyramidal arrangements are markedly distorted. Nonetheless, the structural index parameter proposed by Addison et al.[27] allows us to classify the donor set around the cadmium atoms as trigonal bipyramid rather than a square pyramid (this parameter has a value of 0.76; the values for an idealised trigonal bipyramid and square pyramid are 1 and 0, respectively). It should be noted that pentacoordinate cadmium centres are relatively common, in line with the larger atomic radius of the metal,[28] and has even precedents among structurally characterised complexes featuring simple[29a] and functionalised phosphanes.[29b,29c]

The molecular structure of mercury complex **6** seems, a priori, to be different from **5** as it consists of dimeric $[\{HgBr_2(\mathbf{1}\text{-}\kappa P^2)\}_2]$ units (Figure 7, Table 5) as commonly observed for 1:1 phosphane–mercury(II) halide complexes. However, a closer inspection of the crystal structure reveals the structures to be very similar. The atoms within the cells of both compounds are distributed in a similar manner (see Figure 6), which brings the phosphoryl oxygen O(1) and mercury atoms from neighbouring molecules into proximity [Hg···O = 2.788(2) Å]. Thus, the O(1) atom is capping the {Br(1),Br(2),P(2)} face of a severely distorted tetrahedral donor array formed by phosphane and bromide ligands, although somewhat asymmetrically with respect to the Hg–Br(2^i) axis (*i*: 1 – *x*, –*y*, 1 – *z*), being displaced towards the Br(2)···P(2) edge. As a result, the primary donor set around the mercury atom exhibits severe angular deformation. The protrusion of an extra donor into the coordination sphere of mercury leads to a considerable opening of the Br(2)–Hg–P(2) and, mainly, Br(1)–Hg–P(2) angles (up to about 134° in the latter case), which is compensated by closure of the Br(2)–Hg–Br(2^i) and Br(2^i)–Hg–P(2) angles. It should be noted that in view of the asymmetric "[4+1]" donor environment around the mercury atom, the bonding situation can be described equally well as highly distorted trigonal pyramidal.

The coordination sphere around the mercury atom in **6** is also asymmetric as far as the mercury–donor atom bond lengths are concerned: the three different Hg–Br bond lengths vary by as much as 0.45 Å. As expected, the bond to the terminal bromide Hg–Br(1) is the shortest one while the Hg–Br(2^i) distance is the longest. This clearly points to a competition between the O(1) and Br(2^i) atoms for the coordination site at the mercury.

The bonding situation in solid **7**, yet another isomer of the $[HgBr_2(\mathbf{1})]$ adduct, is more straightforward. The crystal structure (Figure 8, Table 6) consists of discrete centrosymmetric dimers where two phosphanylphosphonate ligands span two $HgBr_2$ units {i.e., **7** can be formulated as $[(\mu\text{-}1\kappa P^2{:}2\kappa O^1\text{-}\mathbf{1})(\mu\text{-}1\kappa O^1{:}2\kappa P^2\text{-}\mathbf{1})(HgBr_2)_2]$}. The coordination sphere around the mercury centres departs slightly from a regular tetrahedron, most likely due to the presence of the sterically encumbered phosphanylferrocene moiety and its orientation towards the {Hg,Br(1),Br(2)} plane: the P(2)–Hg–Br(1,2) angles are less acute, which, in turn, causes a closure of the O(2^{ii})–Hg–Br(1,2) and O(2^{ii})–Hg–P(1) angles (*i*: –*x*, 2 – *y*, –*z*). However, the deformation is much less pronounced than in **6**. The Hg–Br distances in **7** are very similar and do not differ much from the remaining Hg–

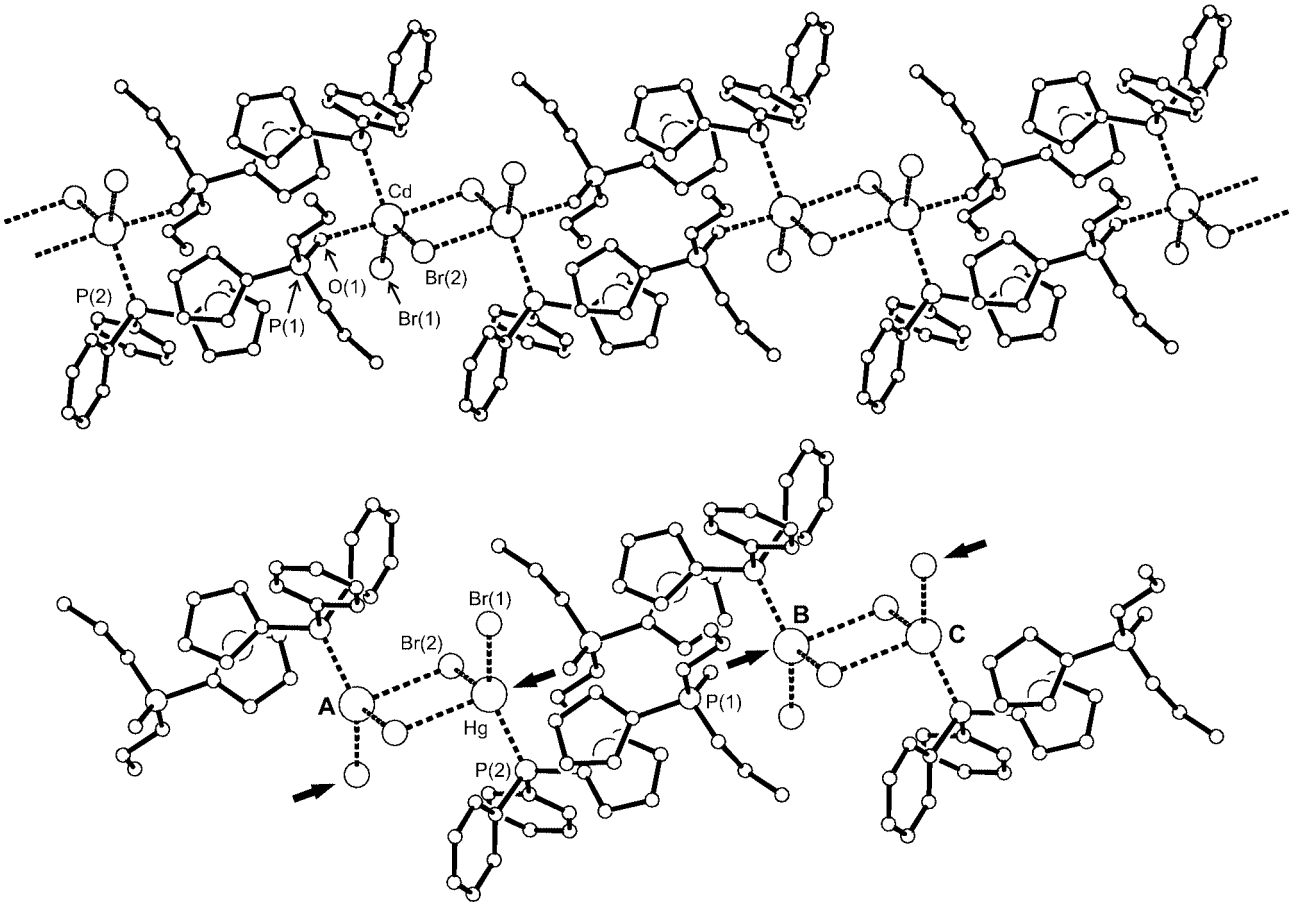

Figure 6. Views of the individual polymeric chain in the structure of **5** (top) and a part of the linear assembly of the dimeric molecules of **6** in the solid state, emphasising the similarity of both structures [intermolecular Hg···O contacts are indicated with arrows; symmetry operations: **A**: 1 – *x*, –*y*, 1 – *z*; **B**: 1 – *x*, 1 – *y*, 1 – *z*; **C**: *x*, 1 + *y*, *z*]. Hydrogen atoms and solvate molecules have been omitted to avoid complicating the figure.

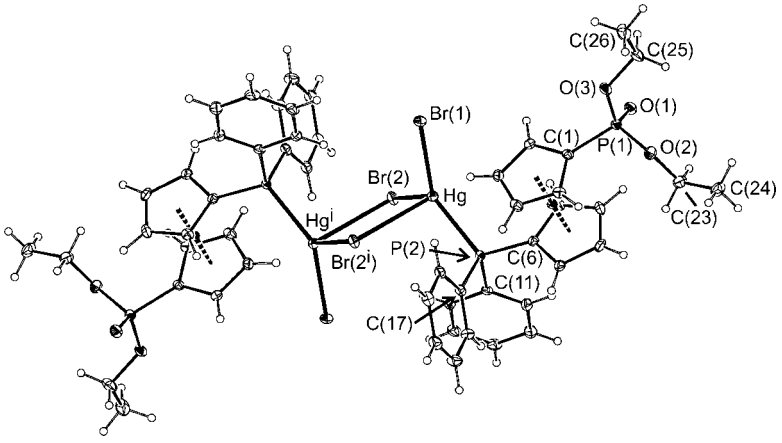

Figure 7. A view of the molecular structure of complex **6** as determined for the solvate **6**·5C_6H_6 (solvent molecules have been omitted for clarity). The dimeric molecule is perfectly centrosymmetric due to the imposed symmetry: the halves lie across the crystallographic inversion centre that coincides with the midpoint of the central {Hg_2Br_2} ring. Displacement ellipsoids are drawn with 30% probability. Symmetry operations: *i*: 1 – *x*, –*y*, 1 – *z*.

donor bond lengths (compare with **6**). Remarkably, the Hg–O(1^{ii}) distance in **7** is only about 5% shorter than that in **6**.[30]

A comparison of the structures determined for the free and several forms of coordinated ligand **1** reveals that coordination of the ligand moiety does not alter its structure in any significant way. The P=O bond lengths are practically identical in all compounds regardless of whether the phosphonate group is free or bonded to a metal (the relative elongation accompanying the coordination is typically less

Table 5. Selected bond lengths [Å] and angles [°] for **6**·5 C_6H_6.[a]

Hg–Br(1)	2.5362(5)	Br(1)–Hg–Br(2)	105.48(1)
Hg–Br(2)	2.6523(4)	Br(1)–Hg–Br(2^i)	100.76(1)
Hg–Br(2^i)	2.9858(4)	Br(1)–Hg–P(2)	134.49(3)
Hg–P(2)	2.4342(9)	Br(2)–Hg–Br(2^i)	83.85(1)
P(1)–O(1)	1.472(3)	Br(2)–Hg–P(2)	118.95(3)
P(1)–O(2)	1.578(3)	Br(2^i)–Hg–P(2)	93.59(2)
P(1)–O(3)	1.571(4)	Hg–Br(2)–Hg^i	96.15(1)
P(1)–C(1)	1.776(4)	O–P(1)–O[b]	102.3(2)–115.3(2)
P(2)–C[c]	1.791(4)–1.824(3)	C–P(2)–C[d]	104.2(2)–106.1(2)
Fe–Cg(1)	1.657(2)	∠Cp(1),Cp(2)	1.0(2)
Fe–Cg(2)	1.654(2)	τ(1)[e]	–155.9(2)

[a] Definitions of the ring planes: Cp(1) C(1–5), Cp(2) C(6–10); Cg(*i*) denotes the respective ring centroid. Symmetry operation used to generate equivalent positions: *i*: 1 – *x*, –*y*, 1 – *z*. [b] The range of O(1)–P(1)–O(2,3) and O(2)–P(1)–O(3) angles. [c] The range of P(2)–C(6,11,17) bonds lengths. [d] The range of C(6)–P(2)–(11,17) and C(11)–P(2)–C(17) angles. [e] Torsion angle C(1)–Cg(1)–Cg(2)–C(6).

Table 6. Selected bond lengths [Å] and angles [°] for **7**.[a]

Hg–Br(1)	2.5939(6)	Br(1)–Hg–Br(2)	110.10(2)
Hg–Br(2)	2.5692(7)	Br(1)–Hg–P(2)	127.60(3)
Hg–P(2)	2.446(2)	Br(1)–Hg–O(1^i)	99.8(1)
Hg–O(1^i)	2.638(4)	Br(2)–Hg–P(2)	122.14(4)
P(1)–O(1)	1.468(5)	Br(2)–Hg–O(1^i)	89.06(9)
P(1)–O(2)	1.574(5)	P(2)–Hg–O(1^i)	86.4(1)
P(1)–O(3)	1.571(5)	O–P(1)–O[b]	102.2(2)–115.6(2)
P(1)–C(1)	1.777(5)	C–P(2)–C[c]	104.2(3)–106.0(3)
P(2)–C[d]	1.799(5)–1.813(6)		
Fe–Cg(1)	1.654(3)	∠ Cp(1),Cp(2)	0.3(3)
Fe–Cg(2)	1.645(3)	τ(1)[e]	155.2(5)

[a] Definitions of the ring planes: Cp(1) C(1–5), Cp(2) C(6–10); Cg(*i*) are the respective ring centroids. Symmetry operation used to generate equivalent positions: *i*: –*x*, 2 – *y*, –*z*. [b] The range of O(1)–P(1)–O(2,3) and O(2)–P(1)–O(3) angles. [c] The range of C(6)–P(2)–(11,17) and C(11)–P(2)–C(17) angles. [d] The range of P(2)–C(6,11,17) bonds lengths. [e] Torsion angle C(1)–Cg(1)–Cg(2)–C(6).

than 1%). Likewise, the O–P–O angles at the phosphonate group do not change upon coordination; in all the structures determined, the O(1)–P(1)–O(2,3) angles are about 10–15° less acute than the remaining angle O(2)–P(1)–O(3). On the other hand, the coordination of the diphenylphosphanyl moiety leads to a slight opening of the C–P(2)–C angles, which thus approach values closer to the tetrahedral ones, albeit without influencing the P(2)–C bond lengths in any significant manner.

More importantly, coordination causes conformational changes to the ferrocene framework. In the free ligand as well and in the complexes, where it acts as an O,P bridge in a discrete dimer (**7**), a polymeric chain (**5**), and in a supramolecularly interacting assembly (**6**), the 1,1′-disubstituted ferrocene unit adopts a conformation between *syn*-eclipsed (τ = 144°) and *anti*-staggered (τ = 180°), with the torsion angles falling in the very narrow range of 155–156°.[31] On the other hand, the P^2-monodentate ligands in hydrated **2** and **3**·4 $CHCl_3$ have the donor groups rotated towards each other, as indicated by τ values of 103/92° (for ligand moieties 1/2) and about 136°, respectively. Chelate coordination of **1** in the zinc(II) complex **4** brings the donor groups even further into proximity, which is reflected by the τ values of around 53° and 60° for molecules 1 and 2, respectively, indicating an intermediate conformation between *syn*-staggered (36°) and *syn*-eclipsed (72°) for the ferrocene unit.

Conclusions

In summary, organometallic phosphanylphosphonate **1**, which is accessible in good yield by sequential metallation/functionalisation of 1,1′-dibromoferrocene, is a typical example of a hybrid ligand that is novel to ferrocene chemistry. In palladium(II) complexes it binds predominantly through the phosphanyl group. However, the participation

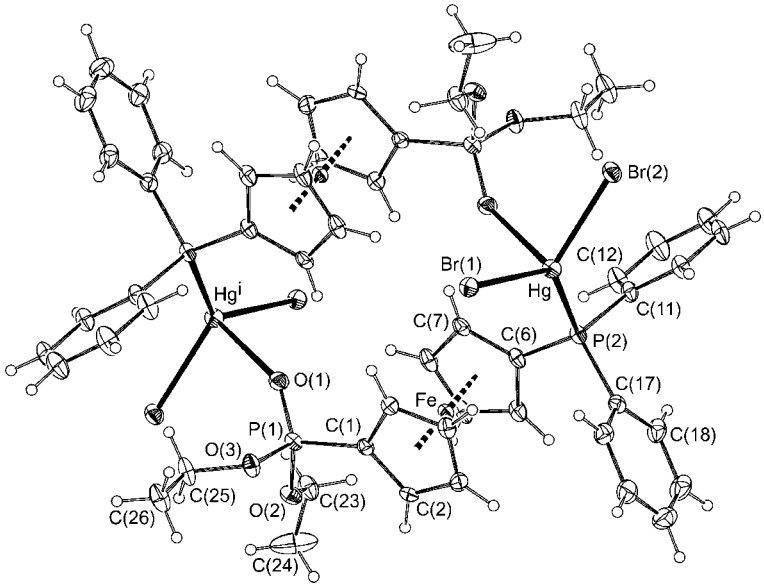

Figure 8. Molecular structure of compound **7**. Similarly to **6**, the parts of the dimeric structure are related by a crystallographic inversion operation. Displacement ellipsoids are shown with 30% probability.

in coordination of the hard phosphonate group can be triggered by increasing the hardness of the ligated metal. This is exemplified by the crystal structures of group-12 metal complexes **4**–**7**, where the increasing hardness of the metal cation results in an increase of the role of $O^1 \rightarrow M$ dative bonding. The hybrid nature of **1** is reflected also by the behaviour of "[$HgBr_2$(**1**)]" in solution: the presence of a weakly coordinating group (phosphonate) renders this adduct structurally fluxional and also allows for isolation of isomeric complexes (**6** and **7**).

It should be pointed out that the direct structural (crystallographic) data discussed in this paper represent the most complete series available thus far for a single phosphanylphosphonate ligand.[32] The data not only demonstrate the flexible nature of **1** as a ligand in the individual molecules of the complexes but also its potential to act as a building block in supramolecular coordination structures. Further investigations into the coordination properties of **1** aimed at new structural motifs are currently underway.

Experimental Section

Materials and Methods: The synthesis of **1** was carried out under argon using tetrahydrofuran (THF) freshly distilled from potassium-benzophenone ketyl. The complexes were synthesised in argon-flushed vessels with exclusion of direct daylight. Chloroform and benzene were dried with anhydrous potassium carbonate and potassium, respectively. Acetone was dried with phosphorus pentoxide, distilled, and stored over activated molecular sieves (4 Å). 1-Bromo-1′-(diphenylphosphanyl)ferrocene was prepared from 1,1′-dibromoferrocene as reported in the literature.[7a] Other chemicals (Lachema, Fluka) and solvents used for crystallisations (methanol, diethyl ether and hexane; Lachema) were used as received.

NMR spectra were recorded with a Varian Unity Inova spectrometer (^{1}H: 399.95; ^{13}C: 100.58; ^{31}P: 161.90 MHz) at 25 °C (unless noted otherwise). Chemical shifts (δ, ppm) are given relative to internal tetramethylsilane (^{13}C and ^{1}H) or to external 85% aqueous H_3PO_4 (^{31}P). The phosphorus-substituted cyclopentadienyl rings represent AA′BB′X spin systems (A, B = ^{1}H, X = ^{31}P), which give rise to characteristic non-binomial multiplets in the ^{1}H NMR spectra. Hence, the multiplicity of the signals of these magnetically nonequivalent protons is given as virtual triplet (vt) or virtual quartet (vq). A similar notation is used for virtual triplets occurring in the ^{13}C{^{1}H} NMR spectrum of **3**. Note: the J' values given below represent an average of the $^{(n)}J_{P,C}$ and $^{(n+2)}J_{P,C}$ coupling constants in the ABX spin system ^{12}C-^{31}P(*A*)-(metal)-^{31}P(*B*)-^{13}C(*X*).[16] IR spectra were measured with an FT IR Nicolet Magna 650 (all compounds in the range 4000–400 cm^{-1}, the complexes also in the far-IR region: 600–100 cm^{-1}). Positive-ion electron impact (EI) and fast atom bombardment (FAB) mass spectra were measured with a ZAB SEQ spectrometer. Electrospray (ESI) mass spectra were recorded with a Bruker Esquire 3000 spectrometer; the samples were dissolved in methanol or firstly in a little chloroform and then diluted with a large excess of methanol.

Diethyl [1′-(Diphenylphosphanyl)ferrocenyl]phosphonate (1): Butyllithium (2.4 mL 2.5 M in hexanes, 6 mmol) was slowly added to a stirred solution of 1-bromo-1′-(diphenylphosphanyl)ferrocene (2.25 g, 5.0 mmol) in THF (50 mL) at –80 °C (temperature in bath). The mixture, which darkened somewhat during the addition, was stirred for another 30 min at the same temperature and then treated with diethyl chlorophosphate (0.9 mL, 6 mmol). The resulting yellow-brown solution was stirred for another 15 min at –80 °C and then for 3 h at room temperature. The mixture was evaporated under reduced pressure and the resulting orange-brown oil (containing precipitated LiCl) was purified by column chromatography on alumina with chloroform/diethyl ether (2:3) as the eluent. The first fraction containing mostly (diphenylphosphanyl)ferrocene was discarded and the second, major band was collected and carefully evaporated under vacuum to give **1** as a viscous, amber oil, which crystallised upon standing at +4 °C. Yield: 2.185 g (86%). ^{1}H NMR ($CDCl_3$): δ = 1.30 (t, $^3J_{H,H}$ = 7.1 Hz, 6 H, CH_3), 4.03–4.14 (m, 4 H, OCH_2), 4.21 (vt, 2 H), 4.26 (d of vt, 2 H), 4.39 (vq, 2 H), 4.58 (vt, 2 H) (fc), 7.29–7.38 (m, 10 H, PPh_2) ppm. ^{13}C{^{1}H} NMR ($CDCl_3$): δ = 16.44 (d, $^3J_{P,C}$ = 7 Hz, CH_3), 61.73 (d, $^2J_{P,C}$ = 6 Hz, OCH_2), 67.59 (d, $^1J_{P,C}$ = 215 Hz, CP^V of fc), 72.29 (d, $J_{P,C}$ = 15 Hz), 72.92 (dd, $J_{P,C}$ = 14 and 1 Hz), 73.39 (d, $J_{P,C}$ = 4 Hz), 74.26 (d, $J_{P,C}$ = 14 Hz) (4 × CH of fc), 77.70 (d, $^1J_{P,C}$ = 8 Hz, CP^{III} of fc), 128.19 (d, $J_{P,C}$ = 7 Hz), 128.62, 133.44 (d, $J_{P,C}$ = 20 Hz) (3 × CH of PPh_2), 138.60 (d, $^1J_{P,C}$ = 10 Hz, C_{ipso} of PPh_2) ppm. ^{31}P{^{1}H} NMR ($CDCl_3$): δ = –17.0 (P^{III}), +25.7 (P^V) ppm. IR (neat): $\tilde{\nu}$ = 3069 (m), 3052 (m), 2981 (s), 2903 (m) ν(C–H); 1478 (s), 1434 (s), 1389 (s), 1369 (m), 1249 (vs), 1188 (s), 1162 (m), 1096 (m), 1050 (vs), 1030 (vs), 961 (vs), 831 (s), 794 (m), 746 (s), 699 (s), 595 (s), 492 (s), 454 (m) cm^{-1}. EI MS: *m*/*z* (%) = 507 (25), 506 (100) [$M^{+\cdot}$], 449 (5) [M – C_4H_9]$^+$ or [M – C_2H_5 – C_2H_4]$^+$, 321 (12) (possibly [$FeC_5H_4POPh_2$]$^+$; see ref.[33]), 226 (6), 225 (18), 201 (19), 198 (6), 197 (5), 183 (35), 171 (16), 170 (10), 141 (5), 133 (8), 121 (14), 119 (13), 56 (5). HRMS calcd. for $C_{26}H_{28}{}^{56}FeO_3P_2$: 506.0863; found 506.0860.

Preparation of *trans*-[{Pd(μ-Cl)Cl(1-κ*P*^{2})}$_2$] (2): Solid [$PdCl_2$(cod)] (57 mg, 0.20 mmol) and **1** (107 mg, 0.21 mmol) were mixed with methanol (3 mL). The solids quickly dissolved to give a burgundy-red solution. The mixture was stirred at room temperature for 90 min and then allowed to stand at –18 °C for several days. The separated microcrystalline solid was filtered off, washed with diethyl ether and dried under vacuum. Yield: 105 mg (76%) of dark red-brown solid (the product typically contains traces of **2** detectable in the ^{31}P NMR spectrum). A crystal selected directly from the reaction mixture (prior to the isolation) was shown to be the solvate **2**·½H_2O. ^{1}H NMR ($CDCl_3$): δ = 1.33 (t, $^3J_{H,H}$ = 7.1 Hz, 6 H, CH_3), 4.07–4.20 (m, 4 H, OCH_2), 4.70 (vq, 2 H), 4.76 (vq, 4 H), 4.81 (vq, 2 H), 5.27 (br. s, 2 H) (fc), 7.34–7.65 (m, 10 H, PPh_2) ppm. ^{13}C{^{1}H} NMR ($CDCl_3$): δ = 16.49 (d, $^3J_{P,C}$ = 6 Hz, CH_3), 62.03 (d, $^2J_{P,C}$ = 6 Hz, OCH_2), 68.96 (very br. d, $^1J_{P,C} \approx$ 210 Hz, CP^V of fc), 70.22 (d, $^1J_{P,C}$ = 67 Hz, CP^{III} of fc), 73.59 (d, $J_{P,C}$ = 15 Hz), 74.35 (d, $J_{P,C}$ = 9 Hz), 75.89 (d, $J_{P,C}$ = 13 Hz), approx. 76.97 (d, $J_{P,C} \approx$ 10 Hz, CH of fc; partly obscured by the solvent signal), 128.23 (d, $J_{P,C}$ = 6 Hz, CH of PPh_2), 128.34 (d, $^1J_{P,C}$ = 61 Hz, C_{ipso} of PPh_2), 134.69 (d, $J_{P,C}$ = 2 Hz), 133.70 (d, $J_{P,C}$ = 12 Hz, CH of PPh_2) ppm. ^{31}P{^{1}H} NMR ($CDCl_3$): δ = +24.6 (P^V), +31.1 ppm (P^{III}) (tentative assignment). IR (Nujol): $\tilde{\nu}$ = 1246 (m), 1184 (m), 1166 (m), 1100 (m), 1027 (vs), 969 (m), 956 (m), 842 (w), 753 (m), 692 (m), 594 (m), 545 (m), 522 (m), 480 (s) cm^{-1}. Far-IR (polyethene): $\tilde{\nu}$ = 356 (s), 350 (sh), 258 (s), 147 (m), 229 (w), 155 (w) cm^{-1}. ESI MS: *m*/*z* = 933, 647 [Pd(**1**)Cl]$^+$. $C_{52}H_{56}Cl_4Fe_2O_6P_4Pd_2$ (1367.3): calcd. C 45.68, H 4.13; found C 45.24, H 4.17.

Preparation of *trans*-[$PdCl_2$(1-κ*P*^{2})$_2$] (3): Neat **1** (112 mg, 0.22 mmol) was added to a suspension of [$PdCl_2$(cod)] (29 mg, 0.10 mmol) in chloroform (4 mL). The yellow complex quickly dissolved to give a red solution, which was allowed to stand for 30 min at room temperature and was then layered with hexane (ca. 10 mL) and allowed to crystallise at 0 °C for several days to afford **2** as an orange, crystalline solid. The complex forms solvates with varying chloroform content: the crystals isolated directly from the mother

liquor and immediately analysed by X-ray diffractions were shown to be the solvate **3**·4 $CHCl_3$. The main portion of the crystalline product, which was isolated by filtration, washed with a little hexane and dried in air, was characterised as **3**·3 $CHCl_3$ (114 mg, 74%; orange crystals). ^1H NMR ($CDCl_3$): δ = 1.30 (td, $^3J_{H,H}$ = 7.1, $^4J_{P,H}$ = 0.5 Hz, 6 H, CH_3), 4.02–4.15 (m, 4 H, OCH_2), 4.58 (vq, 2 H), 4.66 (s, 4 H), 4.89 (d of vt, 2 H) (fc), 7.34–7.62 (m, 10 H, PPh_2) ppm. $^{13}C\{^1H\}$ NMR ($CDCl_3$): δ = 16.45 (d, $^3J_{P,C}$ = 7 Hz, CH_3), 61.85 (d, $^2J_{P,C}$ = 6 Hz, OCH_2), 68.33 (d, $^1J_{P,C}$ = 214 Hz, CP^V of fc), 72.83 (vt, J' = 27 Hz, CP^{III} of fc), 72.95 (d, $J_{P,C}$ = 15 Hz, CH of $C_5H_4P^V$), 74.35 (vt, J' = 4 Hz, CH of $C_5H_4P^{III}$), 74.92 (d, $J_{P,C}$ = 13 Hz, CH of $C_5H_4P^V$), 76.70 (m, CH of $C_5H_4P^{III}$; obscured by the solvent signal), 127.84 (vt, J' = 5 Hz), 130.43 (2 × CH of PPh_2), 130.90 (vt, J' = 25 Hz, C_{ipso} of PPh_2), 134.11 (vt, J' = 6 Hz, CH of PPh_2) ppm. $^{31}P\{^1H\}$ NMR ($CDCl_3$): δ = +15.3 (P^{III}), +25.1 (P^V) ppm. IR (Nujol): $\tilde{\nu}$ = 1248 (s), 1179 (s), 1169 (s), 1096 (m), 1056 (s), 1030 (vs), 965 (vs), 836 (m), 797 (m), 745 (s), 692 (m), 592 (m), 504 (s) cm^{-1}. Far-IR (polyethene): $\tilde{\nu}$ = 354 (m), 189 (w) cm^{-1}. ESI MS: *m/z* = 1211/1213 $[M + Na]^+$, 1153/1155 $[M - Cl]^+$, 1119/1121 $[Pd(\mathbf{1}) + H]^+$, 861 $[Pd(\mathbf{1})_2 - FeC_5H_4PO_3Et_2]^+$. $C_{52}H_{56}Cl_2Fe_2O_6P_4Pd$·3 $CHCl_3$ (1654.5): calcd. C 42.67, H 3.84; found C 42.71, H 3.82.

Preparation of [$ZnBr_2$(1-κ$^2O^1$,P^2)] (4): Phosphonate **1** (58 mg, 0.11 mmol) and anhydrous zinc(II) bromide (23 mg, 0.10 mmol) were dissolved in acetone (2 mL). The resulting orange solution was stirred for one day and then allowed to crystallise by diffusion of diethyl ether vapour. Well-developed orange crystals of the product, which formed during several days, were filtered off, washed with hexane and dried under reduced pressure. Yield: 52 mg (71%). ^1H NMR ($CDCl_3$): δ = 1.41 (td, $^3J_{H,H}$ = 7.0, $^4J_{P,H}$ = 0.7 Hz, 6 H, CH_3), 4.26–4.37 (m, 4 H, OCH_2 and CH of fc), 4.45 (ddq, *J* = 7.8, 9.9 Hz, $^3J_{H,H}$ = 7.0 Hz, 2 H, OCH_2), 4.56 (vq, 2 H), 4.65 (d of vt, 2 H), 4.79 (vq, 2 H) (fc), 7.39–7.71 (m, 10 H, PPh_2) ppm. $^{13}C\{^1H\}$ NMR ($CDCl_3$): δ = 16.19 (d, $^3J_{P,C}$ = 7 Hz, CH_3), 64.46 (d, $^1J_{P,C}$ = 223 Hz, CP^V of fc), 64.61 (d, $^2J_{P,C}$ = 6 Hz, OCH_2), 69.19 (d, $^1J_{P,C}$ = 42 Hz, CP^{III} of fc), 72.83 (d, $J_{P,C}$ = 15 Hz), 73.37 (d, $J_{P,C}$ = 7 Hz), 73.62 (d, $J_{P,C}$ = 16 Hz), 75.52 (d, $J_{P,C}$ = 11 Hz) (CH of fc), 128.88 (d, $J_{P,C}$ = 7 Hz, CH of PPh_2), 129.37 (d, $^1J_{P,C}$ = 38 Hz, C_{ipso} of PPh_2), 131.06 (d, $J_{P,C}$ = 2 Hz), 133.74 (d, $J_{P,C}$ = 13 Hz) (CH of PPh_2) ppm. $^{31}P\{^1H\}$ NMR ($CDCl_3$): δ = –19.9 (d, $^3J_{P,P}$ = 5 Hz, P^{III}), +26.1 (d, $^3J_{P,P}$ = 5 Hz, P^V). IR (Nujol): $\tilde{\nu}$ = 1212 (s), 1177 (s), 1100 (m), 1027 (vs), 983 (w), 966 (w), 845 (w), 828 (m), 813 (m), 754 (m), 743 (m), 694 (m), 592 (s), 489 (s), 466 (s) cm^{-1}. Far-IR (polyethene): $\tilde{\nu}$ = 356 (m), 317 (m), 317 (m), 2351 (s), 244 (s), 219 (s) cm^{-1}. ESI MS: *m/z* = 651 $[Zn(\mathbf{1})Br]^+$, 529 $[\mathbf{1} + Na]^+$. $C_{26}H_{28}Br_2FeO_3P_2Zn$ (731.50): calcd. C 42.69, H 3.86; found C 42.68, H 3.76.

Preparation of [$CdBr_2$(1-κ^2O,P^2)] (5): Phosphonate **1** (56 mg, 0.11 mmol) and $CdBr_2$·4 H_2O (35 mg, 0.10 mmol) were suspended in a mixture of acetone (2 mL) and methanol (1 mL), and the reaction mixture was stirred for 1 d. The solids quickly dissolved to give a clear, orange solution. Crystallisation and isolation as above afforded **5** as an orange, crystalline solid (64 mg, 82%). IR (Nujol): $\tilde{\nu}$ = 1212 (vs), 1178 (vs), 1095 (m), 1067 (m), 1047 (m), 1022 (vs), 982 (m), 964 (m), 837 (w), 795 (w), 751 (s), 697 (s), 591 (s), 498 (s), 486 (m), 458 (w), 442 (w) cm^{-1}. Far-IR (polyethene): $\tilde{\nu}$ = 367 (m), 336 (m), 321 (m), 266 (m), 254 (m), 214 (w), 193 (s), 158 (s), 116 (m) cm^{-1}. ESI MS: *m/z* = 699 $[Cd(\mathbf{1})Br]^+$, 529 $[\mathbf{1} + Na]^+$. $C_{26}H_{28}CdBr_2FeO_3P_2$ (778.52): calcd. C 40.11, H 3.63; found C 40.04, H 3.62.

Reaction of $HgBr_2$ with 1 to Form 6: A mixture of phosphonate **1** (57 mg, 0.11 mmol), $HgBr_2$ (36 mg, 0.10 mmol) and acetone (2 mL) was stirred at room temperature. The solids dissolved quickly to give a clear, orange solution, which immediately deposited a yellow precipitate. After stirring for 30 min, the mixture was transferred to a freezer and allowed to stand at –18 °C overnight. The separated solid was filtered off, washed with diethyl ether (3 × 2 mL) and dried under vacuum. Yield of **6**: 75 mg (87%) of a yellow, powdery solid. A similar reaction in benzene as the solvent (3 mL) gave the microcrystalline solvate **6**·5 C_6H_6, which quickly decomposes in air by losing solvent. Crystals suitable for X-ray measurements were taken directly from the reaction and covered with paraffin oil to prevent their decomposition. The selected specimen was fixed onto a glass fibre with wax and transferred to the diffractometer (see also X-ray crystallography below). ^1H NMR ($CDCl_3$): δ = 1.29 (t, $^3J_{H,H}$ = 7.1 Hz, 6 H, CH_3), 4.00–4.14 (m, 4 H, OCH_2), 4.47 (vq, 2 H), 4.69 (d of vt, 2 H), 4.77 (br. vq, 2 H), 4.86 (br. vt, 2 H) (fc), 7.52–7.79 (m, 10 H, PPh_2) ppm. $^{13}C\{^1H\}$ NMR ($CDCl_3$): δ = 16.42 (d, $^3J_{P,C}$ = 7 Hz, CH_3), 62.05 (d, $^2J_{P,C}$ = 6 Hz, OCH_2), 68.11 (d, $^1J_{P,C}$ = 60 Hz, CP^{III} of fc), 69.11 (d, $^1J_{P,C}$ = 60 Hz, CP^V of fc), 73.34 (d, $J_{P,C}$ = 15 Hz), 74.30 (d, $J_{P,C}$ = 13 Hz), 75.08 (d, $J_{P,C}$ = 13 Hz), 75.94 (d, $J_{P,C}$ = 9 Hz) (CH of fc), 127.71 (d, $^1J_{P,C}$ = 54 Hz, C_{ipso} of PPh_2), 129.55 (d, $J_{P,C}$ = 12 Hz, CH of PPh_2), 132.46 (d, $J_{P,C}$ = 3 Hz), 133.53 (d, $J_{P,C}$ = 13 Hz) (CH of PPh_2) ppm. $^{31}P\{^1H\}$ NMR ($CDCl_3$): δ = 24.3 (s with ^{199}Hg satellites, $^1J_{Hg,P}$ = 6610 Hz, P^{III}), +23.9 (d, $^3J_{P,P}$ = 5 Hz, P^V). Note: the spectra change with the sample concentration (see Table 1). IR (Nujol): $\tilde{\nu}$ = 1225 (s), 1185 (m), 1099 (m), 1065 (m), 1051 (m), 1019 (s), 977 (w), 963 (m), 845 (m), 750 (m), 694 (m), 596 (m), 518 (w), 498 (s), 845 (w), 468 (w) cm^{-1}. Far IR (polyethene): $\tilde{\nu}$ = 343 (w), 316 (w), 264 (w), 254 (m), ν(HgBr) 182 (sh), 176 (s) cm^{-1}. ESI MS: *m/z* = 787 $[Hg(\mathbf{1})Br]^+$, 529 $[\mathbf{1} + Na]^+$. $C_{26}H_{28}Br_2FeHgO_3P_2$ (866.70): calcd. C 36.03, H 3.26; found C 35.95, H 3.24.

Attempted Alkylation of 6. Isolation of 7: Neat methyl iodide (0.31 mL, 5 mmol) was added to a solution of **6** prepared in situ by stirring $HgBr_2$ (36 mg, 0.10 mmol) and **1** (57 mg, 0.11 mmol) in methanol (2 mL) for 15 min. The mixture was stirred for 1 h at room temperature, allowed to stand at 0 °C overnight, and then evaporated under vacuum. The oily residue was dissolved in acetone (ca. 2 mL) and crystallised by gas-phase diffusion of diethyl ether over several days. The crystalline solid formed was filtered off, washed with diethyl ether and dried under vacuum to give **7** as an orange microcrystalline solid. Yield: 81 mg (93%). IR and solution NMR spectra of **7** are identical to those of **6**.

X-ray Crystallography: Crystals suitable for single-crystal X-ray diffraction analysis were selected directly from the reaction batch [**1**: orange plate, 0.08 × 0.25 × 0.50 mm; **4**: orange prism, 0.30 × 0.33 × 0.45 mm; **5**: orange block, 0.15 × 0.20 × 0.20 mm, **6**·5 C_6H_6: fragment of a yellow plate, 0.08 × 0.08 × 0.28 mm (see preparation of this compound above), **7**: orange prism, 0.05 × 0.08 × 0.08 mm] or grown by recrystallisation from chloroform/hexane (**2**·4 $CHCl_3$: orange plate, 0.10 × 0.30 × 0.43 mm). Full-set diffraction data ($\theta \leq 27.5°$) were collected on a Nonius KappaCCD diffractometer equipped with a Cryostream Cooler (Oxford Cryosystems) using graphite-monochromated Mo-K_α radiation (λ = 0.71073 Å) and analysed with the HKL program package.[34] The data were corrected for absorption by using the routines incorporated in the diffractometer software (**1**, **4**, **5**, and **6**·5 C_6H_6: Gaussian correction after indexation of the crystal faces; **2**·4 $CHCl_3$: numerical correction from the indexed crystal shape; **7**: numerical correction based on multiply measured diffractions); transmission factor ranges are given in Table 7. The structures were solved by direct methods (SIR97[35]) and refined by a weighted full-matrix least-squares procedure on F^2 (SHELXL97[36]). All non-hydrogen atoms were refined with anisotropic thermal motion param-

Table 7. Crystallographic data and data-collection and structure-refinement parameters for **2**·4 $CHCl_3$, and **4**–**7**.[a]

Compound	**1**	**2**·4 $CHCl_3$	**4**	**5**	**6**·5 C_6H_6	**7**
Formula	$C_{26}H_{28}FeO_3P_2$	$C_{56}H_{60}Cl_{14}Fe_2O_6P_4Pd$[a]	$C_{26}H_{28}Br_2FeO_3P_2Zn$	$C_{26}H_{28}CdBr_2FeO_3P_2$	$C_{82}H_{86}Br_4Fe_2Hg_2O_6P_4$[b]	$C_{52}H_{56}Br_4Fe_2Hg_2O_6P_4$
M [g mol^{-1}]	506.27	1667.32	731.46	778.49	2123.91	1733.37
Crystal system	triclinic	triclinic	orthorhombic	triclinic	triclinic	triclinic
Space group	$P\bar{1}$ (no. 2)	$P\bar{1}$ (no. 2)	$Pca2_1$ (no. 29)[c]	$P\bar{1}$ (no. 2)	$P\bar{1}$ (no. 2)	$P\bar{1}$ (no. 2)
a [Å]	8.4620(2)	9.2420(2)	19.1144(2)	11.2372(2)	11.3805(3)	11.4381(2)
b [Å]	12.4184(2)	9.6900(1)	17.1194(1)	11.4026(3)	13.1881(2)	11.4585(2)
c [Å]	12.7060(2)	20.6309(4)	17.5230(2)	13.0812(3)	14.8156(4)	12.1543(2)
α [°]	74.290(1)	98.613(1)		70.580(1)	87.526(2)	88.924(1)
β [°]	72.094(1)	90.8192(9)		78.680(1)	73.830(1)	83.964(1)
γ [°]	77.3483(9)	109.896(1)		61.164(1)	68.706(1)	61.7160(8)
Z	2	1	8	2	1	1
V [Å^3]	1209.56(4)	1713.49(5)	5734.00(9)	1383.46(5)	1985.68(8)	1394.14(4)
$D_{calcd.}$ [g mL^{-1}]	1.390	1.616	1.695	1.869	1.776	2.065
T [K]	150(2)	150(2)	150(2)	150(2)	150(2)	150(2)
μ(Mo-K_α) [mm^{-1}]	0.781	1.363	4.267	1.323	6.356	9.027
T[d]	0.747–0.930	0.670–0.859	0.227–0.387	0.367–0.613	0.273–0.664	0.379–0.539
Reflns. total	35528	29888	97688	24724	31669	48178
R_{int} [%][e]	3.93	4.24	5.11	4.05	5.43	7.95
Unique/obsd.[f] reflns.	5556/4944	7818/6733	13125/11869	6346/5734	9106/7962	6395/5095
R (obsd. data) [%][g]	3.55	4.08	2.67	2.55	3.00	3.59
R, wR (all data)[%][g]	4.11, 9.89	5.01, 10.3	3.47, 5.27	3.03, 6.19	3.85, 714	5.56, 8.36
$\Delta\rho$ [e Å^{-3}]	1.05, –0.98	1.46, –0.54	1.34, –0.99	1.12, –0.94	0.98, –2.03	1.37, –1.74

[a] $(C_{52}H_{56}Cl_2Fe_2O_6P_4Pd)(CHCl_3)_4$. [b] $(C_{26}H_{28}Br_2FeHgO_3P_2)_2(C_6H_6)_5$. [c] Flack's enantiomorph parameter: –0.007(4). [d] The range of transmission coefficients. [e] $R_{int} = \Sigma|F_o^2 - F_o^2(mean)|/\Sigma F_o^2$, where $F_o^2(mean)$ is the average intensity for symmetry-equivalent reflections. [f] Diffractions with $I_o > 2\sigma(I_o)$. [g] $R = \Sigma||F_o| - |F_c||/\Sigma|F_o|$, w$R = [\Sigma\{w(F_o^2 - F_c^2)^2\}/\Sigma w(F_o^2)^2]^{1/2}$.

eters whilst the hydrogen atoms were included in the calculated positions and refined using the riding model. Relevant crystallographic data are given in Table 7. Geometric parameters and structural drawing were produced with a recent version of the Platon program.[37]

CCDC-281044 (for **1**), -281045 (for **2**·½ H_2O), -281046 (for **3**·4 $CHCl_3$), -281047 (for **4**), -281048 (for **5**), -281049 (for **6**·5 C_6H_6), and -281050 (for **7**) contain the supplementary crystallographic data for this paper. These data can be obtained free of charge from The Cambridge Crystallographic Data Centre via www.ccdc.cam.ac.uk/data_request/cif.

Supporting Information (see footnote on the first page of this article): The Supporting Information contains VT ^1H and $^{31}P\{^1H\}$ NMR spectra for **6** (Figures S1 and S2).

Acknowledgments

This work was financially supported by the Grant Agency of the Czech Republic (grant no. 104/05/0192).

[1] a) *Ferrocenes: Homogeneous Catalysis, Organic Synthesis Materials Science* (Eds.: A. Togni, T. Hayashi); VCH, Weinheim, **1995**; b) A. Togni, in *Metallocenes: Synthesis, Reactivity, Applications* (Eds.: A. Togni, R. L. Halterman), Wiley-VCH, Weinheim, **1998**; vol. 2, chapter 11, p. 685; c) T. J. Colacot, *Chem. Rev.* **2003**, *103*, 3101.

[2] R. C. J. Atkinson, V. C. Gibson, N. J. Long, *Chem. Soc. Rev.* **2004**, *33*, 313.

[3] I. R. Butler, W. R. Cullen, T. J. Kim, S. J. Rettig, J. Trotter, *Organometallics* **1985**, *4*, 972.

[4] I. R. Butler, S. J. Coles, M. B. Hursthouse, D. J. Roberts, N. Fujimoto, *Inorg. Chem. Commun.* **2003**, *6*, 760.

[5] a) M. Yamashita, J. V. C. Vicario, J. F. Hartwig, *J. Am. Chem. Soc.* **2003**, *125*, 16347; b) T. Tu, W.-P. Deng, X.-L. Hou, L.-X. Dai, X.-C. Dong, *Chem. Eur. J.* **2003**, *9*, 3073.

[6] a) M. Laly, R. Broussier, B. Gautheron, *Tetrahedron Lett.* **2000**, *41*, 1183; b) J.-C. Hierso, F. Lacassin, R. Broussier, R. Amardeil, P. Meunier, *J. Organomet. Chem.* **2004**, *689*, 766.

[7] a) I. R. Butler, R. L. Davies, *Synthesis* **1996**, 1350; b) V. V. Grushin, *Organometallics* **2001**, *20*, 3950; c) T. S. A. Hor, H. S. O. Chan, K. L. Tan, L. T. Phang, Y. K. Yan, L. K. Liu, Y. S. Wen, *Polyhedron* **1991**, *10*, 2437; d) L. T. Phang, K. S. Gan, H. K. Lee, T. S. A. Hor, *J. Chem. Soc., Dalton Trans.* **1993**, 2697; e) G. Pilloni, B. Longato, G. Bandoli, *Inorg. Chim. Acta* **1998**, *277*, 163; f) R. J. Coyle, Yu. L. Slovokhotov, M. Yu. Antipin, V. V. Grushin, V. Vladimir, *Polyhedron* **1998**, *17*, 3059.

[8] a) G. Pilloni, B. Longato, G. Bandoli, *Inorg. Chim. Acta* **1998**, *277*, 163; b) R. Broussier, E. Bentabet, M. Laly, P. Richard, L. G. Kuzmina, P. Serp, N. Wheatley, P. Kalck, B. Gautheron, *J. Organomet. Chem.* **2000**, *613*, 77.

[9] a) T. S. A. Hor in ref.[1a], chapter 1, p. 3; b) G. Bandoli, A. Dolmela, *Coord. Chem. Rev.* **2000**, *209*, 161.

[10] a) T. L. Schull, D. A. Knight, *Coord. Chem. Rev.* **2005**, *249*, 1269; b) S. R. Alley, W. Henderson, *J. Organomet. Chem.* **2001**, *637–639*, 216 and references cited therein; c) O. Oms, F. Maurel, F. Carré, J. Le Bideau, A. Vioux, D. Leclercq, *J. Organomet. Chem.* **2004**, *689*, 2654.

[11] S. Basra, J. G. de Vries, D. J. Hyett, G. Harrison, K. M. Heslop, A. G. Orpen, P. G. Pringle, K. von der Luehe, *Dalton Trans.* **2004**, 1901.

[12] Crystallographic data for **3**: $C_{52}H_{56}Cl_4Fe_2O_6P_4Pd_2$·½ H_2O (solvating water), triclinic, space group $P\bar{1}$ (no. 2), a = 9.8080(3), b = 16.6990(7), c = 17.2320(8) Å; α = 93.588(2)°, β = 105.485(3)°, γ = 95.326(3)°; V = 2696.9(2) Å^3, Z = 2, μ(Mo-K_α) = 1.550 mm^{-1} (Gaussian absorption correction applied, T range: 0.744–0.940); 36531 total, 9465 unique and 6850 observed [$I_o > 2\sigma(I_o)$] reflections, final R (observed data) = 5.07%; wR (all data) = 13.21%. Atoms in the disordered phosphonate group were refined over two positions (with idealised distances) with isotropic thermal motion parameters. All other heavy atoms were refined anisotropically; hydrogen atoms were included in calculated positions and refined using the riding model (SHELXL97).

[13] CSD version 5.24 (November **2004**) with updates of February and May **2005**.

[14] A search for structural fragments $\{Pd(\mu\text{-}X)X(P)\}_2$, where X is any halide, furnished 36 hits with *R* below 10%. Most of them are planar molecules (mostly due to imposed symmetry) with the dihedral angle, φ, equal or close to 0°. Only four structures exhibit φ higher than 15°; refcode (φ, °): NEHVUR (16.2), QAHNOC (29.2), QIVLEM (38.0 and 41.9, two independent fragments), WAVPOY (16.2); φ is the dihedral angle subtended by the $\{PdX_2P\}$ planes.
[15] The $\Delta\delta_P$ values were calculated from shifts given in ref.[16] (the complexes) and in: S. O. Grim, A. W. Yanowsky, S. A. Bruno, W. J. Bailey, E. F. Davidoff, T. J. Marks, *J. Chem. Eng. Data* **1970**, *15*, 497 (the ligand).
[16] P. S. Pregosin, R. W. Kunz, in *^{31}P and ^{13}C NMR of Transition Metal Phosphane Complexes*, *NMR Basic Principles and Progress* (Eds.: P. Diehl, E. Fluck, R. Kosfeld), Springer, Berlin, **1979**, vol. 16, ch. E, p. 65 and references cited therein.
[17] P. Štěpnička, J. Podlaha, R. Gyepes, M. Polášek, *J. Organomet. Chem.* **1998**, *552*, 293.
[18] Similar reactions with a 2:1 molar ratio gave no defined solid products, possibly due to a higher solubility of the compounds formed.
[19] $[MCl_2(dppf\text{-}\kappa P,P')]$: M ($\Delta\delta_P$) = Zn (–4.5 ppm), Cd (8.1 ppm) and Hg (+36.0 ppm). Data from: B. Corrain, B. Longato, G. Favero, D. Ajò, G. Pilloni, U. Russo, F. R. Kreissl, *Inorg. Chim. Acta* **1989**, *157*, 259.
[20] $[MCl_2(dippf\text{-}\kappa P,P')]$: M ($\Delta\delta_P$) = Zn (–6.6 ppm), Cd (+9.8 ppm) and Hg (+40.3 ppm). The shifts were calculated from the data cited in: a) A. R. Elsagir, F. Gassner, H. Görls, E. Dinjus, *J. Organomet. Chem.* **2000**, *597*, 139; b) J. H. L. Ong, C. Nataro, J. A. Golen, A. L. Rheingold, *Organometallics* **2003**, *22*, 5027.
[21] A. K. S. Chauhan, N. Singh, R. D. Srivastava, *Appl. Organomet. Chem.* **2003**, *17*, 586 and references cited therein.
[22] R. G. Goel, W. P. Henry, N. K. Jha, *Inorg. Chem.* **1982**, *21*, 2551.
[23] G. A. Bowmaker, J. J. Clase, N. W. Alcock, J. M. Kessler, J. H. Nelson, J. S. Frye, *Inorg. Chim. Acta* **1993**, *210*, 107.
[24] R. J. Coyle, Y. L. Slovokhotov, M. Y. Antipitin, V. V. Grushin, *Polyhedron* **1998**, *17*, 3059.
[25] V. C. Gibson, N. J. Long, A. J. P. White, C. K. Williams, *J. Chem. Soc., Dalton Trans.* **2002**, 3280.
[26] D. Drahoňovský, I. Císařová, P. Štěpnička, D. Dvořáková, P. Maloň, D. Dvořák, *Collect. Czech. Chem. Commun.* **2001**, *66*, 588.
[27] A. W. Addison, T. N. Rao, J. Reedijk, J. van Rijn, G. C. Verschoor, *J. Chem. Soc., Dalton Trans.* **1984**, 1349.
[28] The ionic radii for divalent metals with coordination number of six are 0.88 (Zn), 1.09 (Cd) and 1.16 Å (Hg). Besides, cadmium(II), like any other metal ion with a d^{10} configuration, has no preferred coordination geometry due to ligand-field stabilisation. Consequently, the coordination geometries are determined chiefly by interplay of electrostatic forces, the nature of the ligands and steric factors. For a reference see, for example: F. A. Cotton, G. Wilkinson, C. A. Murillo, M. Bochmann, *Advanced Inorganic Chemistry*, 6th ed., Wiley, New York, **1999**, chapter 15, p. 598 ff.
[29] The following structures of phosphane–halide complexes featuring pentacoordinate cadmium(II) centres have been retrieved from the Cambridge Crystallographic Database (version 5.26 of November **2004** with updates from February and May **2005**). None of the above compounds is polymeric; a) N. A. Bell, T. D. Dee, I. W. Nowell, *Inorg. Chim. Acta* **1982**, *65*, L87 (code: BIYDIW); b) L. W. Houk, P. K. S. Gupta, M. B. Hossain, D. van der Helm, *Acta Crystallogr., Sect. B* **1982**, *38*, 91 (code: BAZMIY); c) J. T. Mague, J. L. Krinsky, *Inorg. Chem.* **2001**, *40*, 1962 (code: QIWBON).
[30] Notably, the mercury-to-oxygen distances in **6** and **7** fall between the sum of covalent (2.38 Å) and contact (4.02 Å) radii (atomic radii were taken from the Platon program[37]). The flexibility of Hg←O dative bonding can be accounted for by its relative weakness because a variation of the Hg–O distance will result in relatively low energy changes which can, in turn, be compensated by other operating effects, such as steric factors and crystal packing forces.
[31] See also the discussion of conformations adopted by the related ligand 1′-(diphenylphosphanyl)ferrocenecarboxylic acid in the solid state: P. Štěpnička, *Eur. J. Inorg. Chem.* **2005**, 3787.
[32] According to the CSD,[13] the only other structurally characterised ligand is diethyl 2-(diphenylphosphanyl)phenylphosphonate whereas the complexes featuring this and some related donors whose structures were determined are limited exclusively to those with palladium(II) and platinum(II) and just a few examples for each ligand. Representative examples for diethyl 2-(diphenylphosphanyl)phenylphosphonate: a) D. D. Ellis, G. Harrison, A. G. Orpen, H. Phetmung, P. G. Pringle, J. G. de Vries, H. Oevering, *J. Chem. Soc., Dalton Trans.* **2000**, 67 (ligand and Pt complex); for diethyl 2-(diphenylphosphanyl)-ethylphosphonate: b) S. Ganguly, J. T. Mague, D. M. Roundhill, *Inorg. Chem.* **1992**, *31*, 3500 (Pd complex); for diethyl 3-(diphenylphosphanyl)propylphosphonate: c) G. Guerrero, P. H. Mutin, F. Dahan, A. Vioux, *J. Organomet. Chem.* **2002**, *649*, 113 (Pd and Pt complexes).
[33] M. Polášek, P. Štěpnička, *J. Mass Spectrom.* **1998**, *33*, 739.
[34] Z. Otwinowski, W. Minor, *HKL Denzo and Scalepack Program Package*, Nonius BV, Delft, The Netherlands. For a reference, see: Z. Otwinowski, W. Minor, *Methods Enzymol.* **1997**, *276*, 307.
[35] A. Altomare, M. C. Burla, M. Camalli, G. L. Cascarano, C. Giacovazzo, A. Guagliardi, A. G. G. Moliterni, G. Polidori, R. Spagna, *J. Appl. Crystallogr.* **1999**, *32*, 115.
[36] G. M. Sheldrick, *SHELXL97. Program for Crystal Structure Refinement from Diffraction Data*, University of Göttingen, Germany, **1997**.
[37] A. L.Spek, *Platon, a multipurpose crystallographic tool*, Utrecht University, Utrecht, The Netherlands, **2003** and updates. Distributed via Internet; home page: http://www.cryst.chem.uu.nl/platon/.

Received: August 15, 2005
Published Online: January 16, 2006

